

# CMS Central Hadron Calorimeter

Howard S. Budd<sup>a</sup>

<sup>a</sup>Department of Physics and Astronomy, University of Rochester, Rochester, NY 14627

We present a description of the CMS central hadron calorimeter. We describe the production of the 1996 CMS hadron testbeam module. We show the results of the quality control tests of the testbeam module. We present some results of the 1995 CMS hadron testbeam.

## 1. CMS Central Hadron Calorimeter

The design of the CMS detector starts with the 4 T solenoidal magnet of length 13 m and inner diameter 5.9 m. The magnet determines many of the features of the CMS calorimeters, since the CMS calorimeter is located inside the magnet. Figure 1 shows a quarter slice of the CMS up to the coil. The EM calorimeter, ECAL, consists of lead tungstate, PbWO<sub>4</sub>, crystals. The hadron calorimeter, HCAL, surrounds ECAL. The most important requirement of HCAL is to minimize the non-gaussian tails of the energy resolution function. Hence, HCAL design maximizes as much interaction length of material inside the magnetic coil as possible. Copper absorber satisfies this requirement, as well as being nonmagnetic. In addition, copper is fairly low Z, so it does not degrade the muon momentum measurement. Maximizing the amount of absorber before the magnet requires minimizing the amount of space devoted to active medium. The tile/fiber technology is an ideal choice. It consists of plastic scintillator tiles read out with embedded wave length shifting (WLS) fibers. This technology was first developed by the UA1 collaboration and at Protvino [1]. The system is being used in the upgrade of the CDF endcap calorimeter [2]. It enables HCAL to be easily built with a tower geometry readout. The entire HCAL area can be instrumented with no uninstrumented cracks.

HCAL covers the pseudorapidity range  $|\eta| < 3.0$  with a barrel (central) and endcap hadron calorimeter. The barrel calorimeter covers  $0 < |\eta| < 1.4$ , while the endcap calorimeter covers down to  $|\eta|=3.0$ . The region to  $|\eta|=5.0$  is

covered by a very forward calorimeter. HCAL is segmented into towers of granularity  $\Delta\eta \times \Delta\phi=0.087 \times 0.087$ . This granularity is sufficient for good dijet mass resolution. The rest of this article will only discuss the barrel hadron calorimeter.

HCAL is built as 20° wedges inside the magnet. Figure 2 shows a 20° wedge, with ECAL on the right side and HCAL on the left side. The body of wedges are copper, but the inner and outer plates are stainless steel for structural strength. The wedges are bolted together. This enables the wedges to be assembled cheaply and minimizes the crack between the wedges to  $\leq 2$  mm. The wedges contain 15 active layers segmented into 2 readouts. A space of 9 mm is left for active layers. The HCAL is about 1 meter thick inside the magnet,  $6.2 \lambda$  at  $\eta=0$ . This is not enough material to contain a high energy hadron shower. Hence, 2 layers are instrumented outside the magnet. A layer of scintillator is put after the coil and after the innermost muon steel. This adds an additional  $4 \lambda$  at  $\eta=0$ .

The active medium uses the tile/fiber concept as used by the CDF plug upgrade. The hadron calorimeter consists of about 70,000 individual tiles. In order to limit the number of individual elements, the tiles of a given layer are put into a single mechanical unit called a megatile. Figure 3 displays a typical megatile. The megatile with segmentation of  $16(\eta) \times 2(\phi)$  goes into the  $\phi$  center of a wedge while the megatile with segmentation  $16(\eta) \times 1(\phi)$  goes into the edge slots in a wedge. Each layer has 108 megatiles. Figure 4 shows a cross section of the megatile. The scintillator is surrounded by Tyvek 1073D for reflectiv-

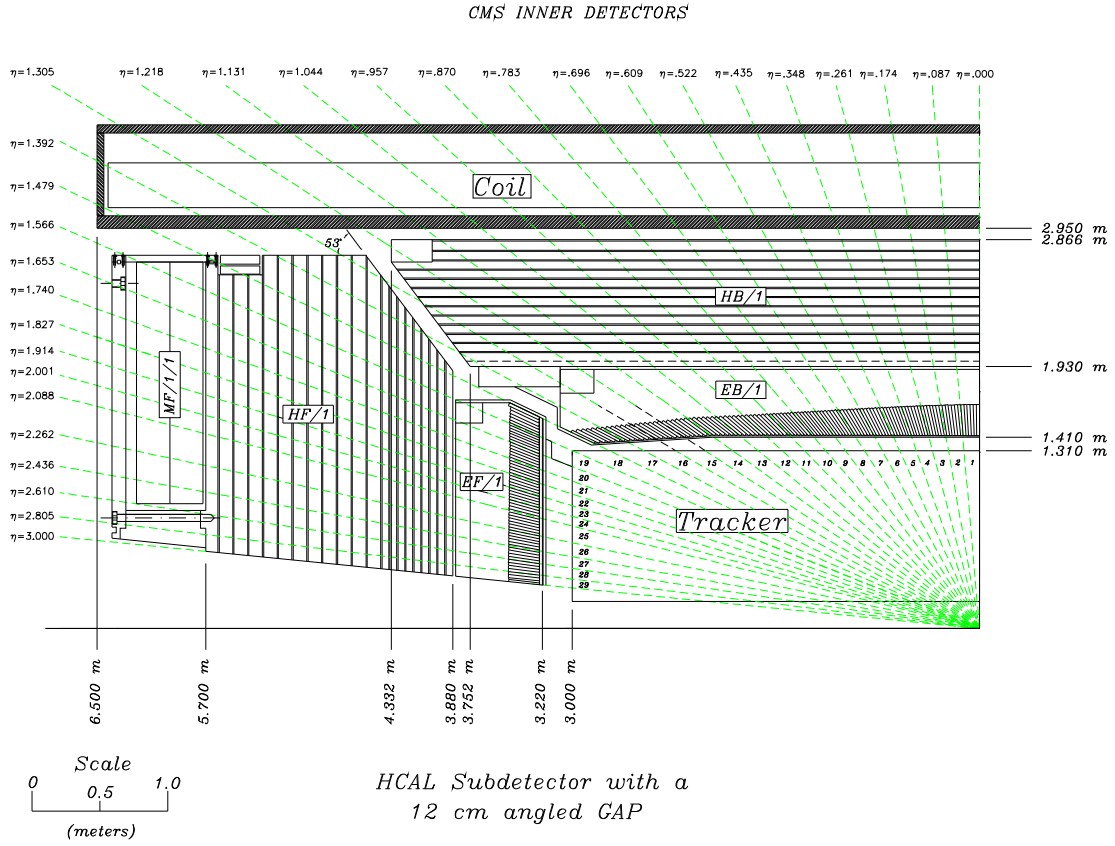


Figure 1. CMS electromagnetic detector, hadronic detector, and solenoidal magnet.

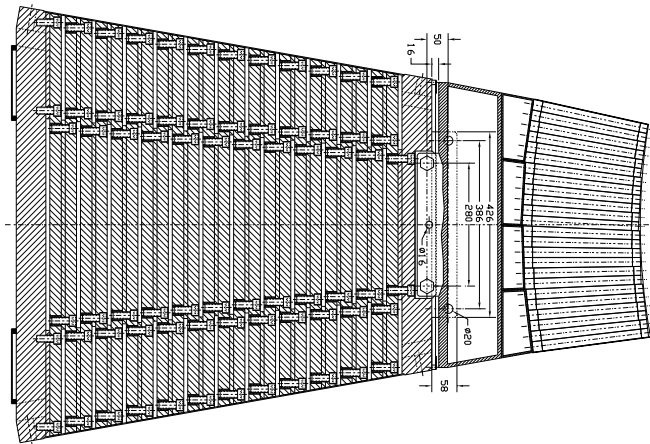


Figure 2. Drawing of 20° wedge.

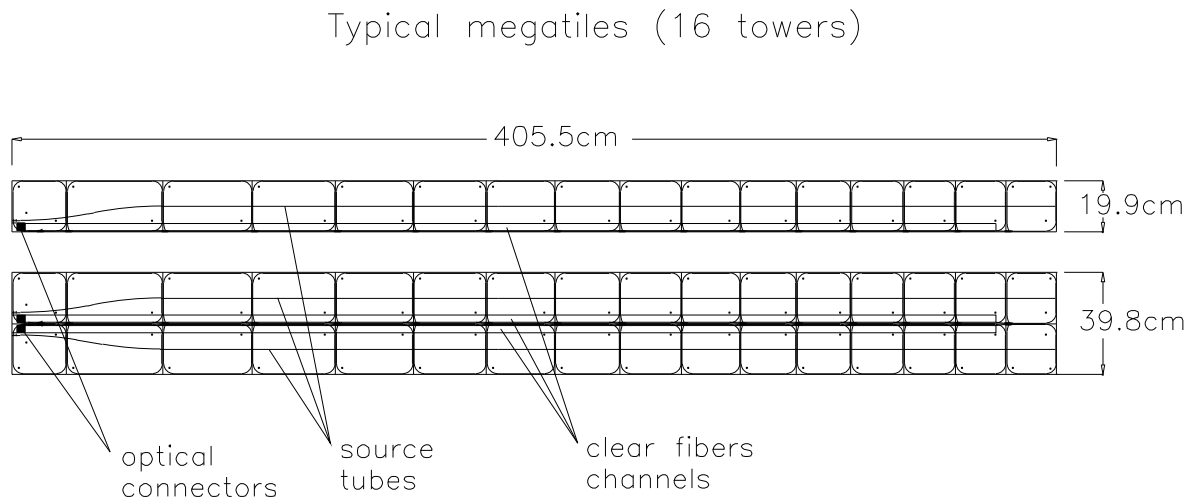


Figure 3. CMS electromagnetic detector, hadronic detector, and solenoidal magnet.

ity. The scintillator and Tyvek are surrounded by tedlar for light tightness. The top plastic routes the fibers and source tubes.

The baseline scintillator is 4 mm Kuraray SCSN81. The scintillator is read out by a WLS fiber, Kuraray multiclاد Y-11 (Fluor K27), embedded in the tile in a  $\sigma$  pattern. Outside the scintillator, the WLS fiber is spliced to Kuraray multiclاد clear fiber. Next, the clear fiber goes to an optical connector at the end of the pan. An optical cable takes the light to an optical descrambler. The descrambler arranges the fibers into readout towers and brings the light to a hybrid photomultiplier tube (HPMT). Since the descrambler will be operating in the 4 T magnetic field, conventional phototubes will not work.

The HPMT consists of a photocathode and a PIN diode separated by  $\sim 1$  mm. The photoelectrons from the photocathode are accelerated to the PIN diode by high voltage,  $\sim 10,000$  volts. The HPMT has a gain of 1000 to 2000. If the electric field is aligned with the magnetic field, they can operate in a magnetic field of 4 T. This makes them suitable for CMS HCAL.

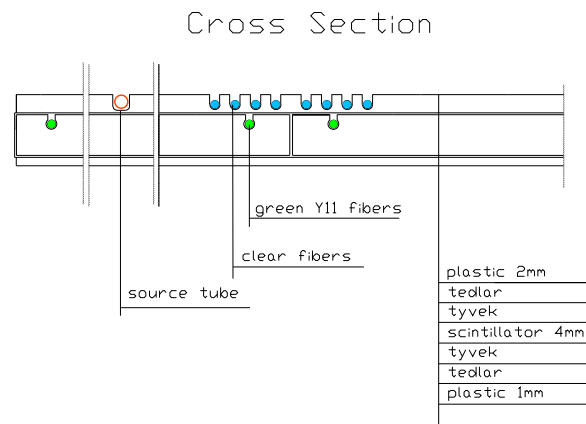


Figure 4. Cross section view of a megatile.

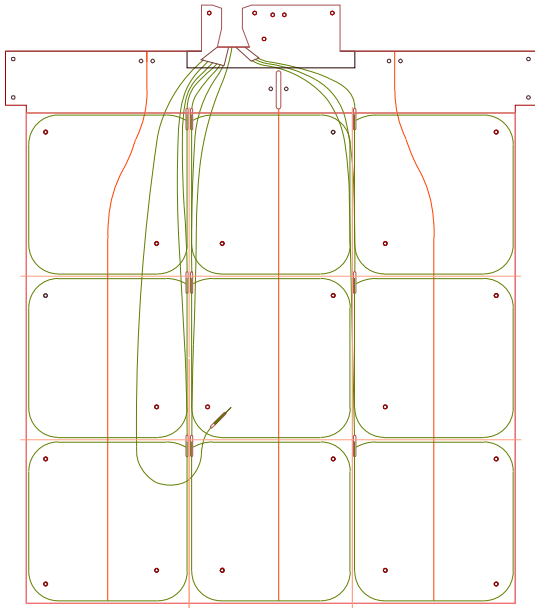


Figure 5. Megatile for 1996 CMS HCAL test-beam.

## 2. CMS hadron calorimeter test beam

We have built modules for a 1995 and 1996 test-beam at CERN. The purpose of the testbeam is to determine the response of the calorimeter in a magnetic field and to determine the resolution of the combined ECAL and HCAL calorimeter. To determine the response in a magnetic field, the calorimeter was put inside the EPS magnet in the H2 beam line at CERN. We describe the calorimeter and its production to illustrate the production of the real device and show some of the quality control tests we will use for the real device. All numbers we quote for the quality control are for the 1996 testbeam module.

### 2.1. 1996 HCAL Testbeam Megatile

Figure 5 shows the megatile for the 1996 test-beam. The active area is 64 cm by 64 cm and consists of 9 separate towers. The transverse size of the testbeam megatile is determined by size of the center of the EPS magnet. Embedded in each

tile is a WLS fiber in the  $\sigma$  pattern. Outside the tile, the WLS fibers are spliced to multicladd clear fibers. The clear fibers are routed out to a connector at the end of the megatile. The fiber on the left going into the middle tile is a light injection fiber. For calibration purposes light is injected into the tile through this fiber. The megatile has 3 thin stainless steel tubes, diameter=1 mm, that will route  $\text{Cs}^{137}$  radioactive sources through the center of each tile. A picoammeter measures the current generated by the source to simultaneously calibrate the tile, fibers, and photodetector.

The elements for the megatile are drawn on a CAD system. The drawings are converted to machine code which can be run on a computer controlled router, a Thermwood machine.

We describe the production and quality control of the device. First the WLS fibers are cut, polished, and mirrored. The reflectivity of the mirror is checked by measuring test fibers which are mirrored along with the fibers used in the calorimeter. Measuring the reflectivity of the mirror gives

$$\text{light}_{\text{with mirror}}/\text{light}_{\text{with mirror cut off}} = 1.85$$

This measurement is done with a computer controlled UV scanner with the fibers read out by pin diodes. Clear fibers are spliced onto WLS fibers with a fusion splicer. The transmission across the splice is checked by splicing a sample of WLS fibers onto WLS fibers. The splice region is measured with the UV scanner. The transmission across the splice is 92.6% with an RMS of 1.8%. Next, the optical fibers are glued into a 10 fiber connector. This configuration is called a pigtail. In order to get the fiber lengths correct, the pigtail is assembled in a templet. The connector is diamond polished. The fibers are measured with the UV scanner. The scanner checks the green fiber, clear fiber, splice, and mirror. The RMS of the light from the fibers is 1.9%.

The pigtail is inserted into the megatile. The completed megatile is checked with an automated source scanner. A  $\text{Cs}^{137}$  source is in a lead collimator. This yields a 4 cm diameter source spot on the megatile. The collimator is moved with a computer controlled x-y motor. From the scanner we determine the relative light yield of each tile and the uniformity of the each megatile. The gain

of the individual tiles has an RMS of 4.6%, while the transverse uniformity of the megatile is 4.5%. A  $\text{Cs}^{137}$  wire source is run through the 3 source tubes and the light yield is measured. The RMS of the ratio of collimated source to wire source is 1.3%. This means the line sources, which can be used when the calorimeter is completely assembled, can calibrate the tiles to better than 1.3%. Fiber cables are constructed separately and tested with the UV scanner.

The testbeam module has several methods to maintain the calibration. As just described, it has small steel tubes to run a wire source. It has a laser and LED light injection system. The photomultiplier tube that reads out the calorimeter has an addition fiber going to it. Either a laser or an LED can inject light into this fiber. During the testbeam we injected light with both the laser and LED. As shown on the drawing of the megatile, there is a fiber which can inject light into a tile. A more complete description of the calibration, including procedures for calibrating the full calorimeter, is given in ref [4].

## 2.2. 1995 HCAL Testbeam Results

We present results from the 1995 testbeam. Results for the 1996 testbeam are not yet final. Figure 6 shows the testbeam configurations. For the Pb/scin ECAL module, ECAL is the 10 layer lead/scintillator sandwich sampling calorimeter, positioned directly upstream of the HCAL. The HCAL corresponds to the end cap configuration (5 cm and 10 cm copper absorber plates in HAC1 and HAC2 respectively). For the  $\text{PbWO}_4$  crystal ECAL module, the ECAL detector ( $7 \times 7$  matrix of 2 cm by 2 cm by 23 cm  $\text{PbWO}_4$  crystals) is followed by the HCAL in the barrel configuration (3 cm and 5 cm copper absorber plates in HAC1 and HAC2 respectively). There is approximately 46 cm air gap between the end of ECAL and the front face of HCAL. Each layer for both configurations is readout by a phototube connected to a 10 m optical cable.

Figure 7 shows the average pion and electron response of the calorimeter, as a function of the B field, relative to the 0 T setting. The data indicates an approximate 6% increase in the response of the calorimeter to pions and electrons

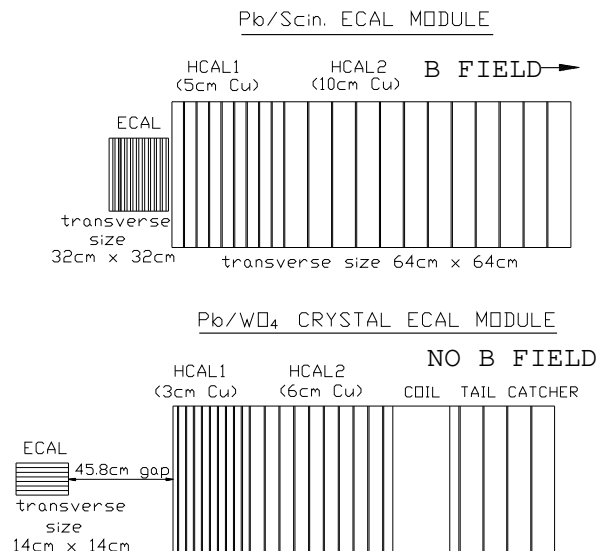


Figure 6. Schematic drawing of the calorimeter modules used during the 1995 test beam.

for B field at 1 T, 2 T, and 3 T. The measurement is consistent with the increased light yield of the scintillator tiles, as measured by the calibration system using the radioactive  $\gamma$  source. The 1996 test beam run had the magnetic field transverse to the beam direction. The result is different if the magnetic field is transverse to the beam direction. A discussion is in ref [4] and will be in future presentations of the 1996 test beam.

The overall calibration constant of the hadron calorimeter is determined by using 50 GeV hadrons, and the overall calibration constant of EM calorimeter is determined using 150 GeV electrons. The total energy of pions is defined as

$$E_{tot}^{pions} = \alpha \times E_{em} + E_{had}$$

where  $\alpha$  is a parameter we vary to study linearity and resolution. Figure 8 shows the linearity of the Pb/scin ECAL configuration for pions which are minimum ionizing (mip) in ECAL and all pions ( $\alpha=1$ ). The energy resolutions for the 2 cases are comparable. The fit of this data to the relative

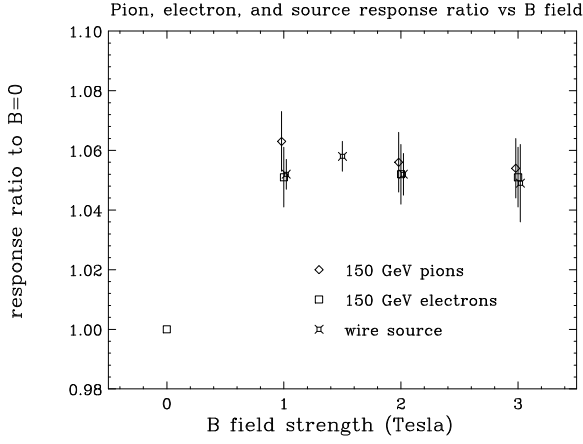


Figure 7. H2 Test Beam results: average pion, average electron, and Cs<sup>137</sup> source response of the calorimeter, as a function of the B field.

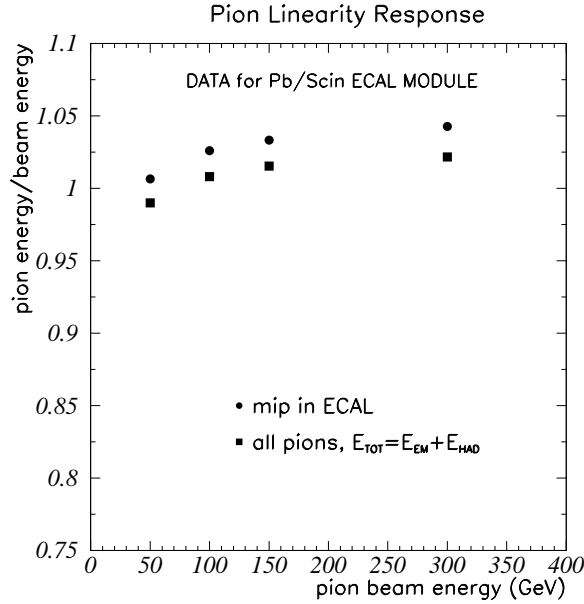


Figure 8. Linearity of Pb/scin ECAL module.

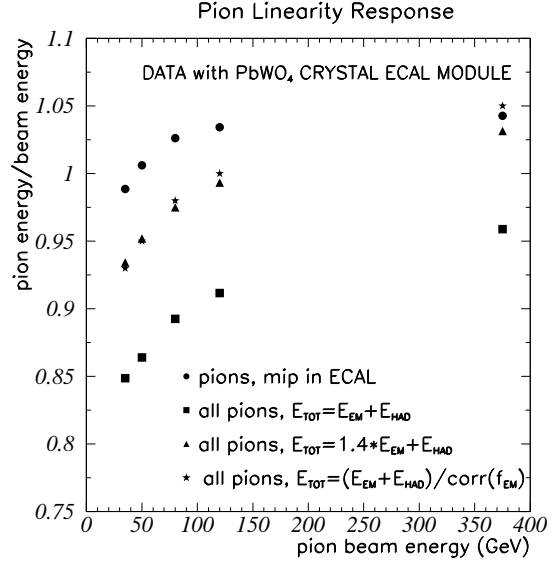


Figure 9. Linearity of PbWO<sub>4</sub> crystal module for hadrons.

energy resolution function is

$$\sigma_E/E = (\text{stoch. term})/\sqrt{E} \oplus (\text{const. term})$$

where stochastic and constant terms are combined in quadrature. For pions which are mip in ECAL we have

$$\sigma_E^{\pi \text{ mip in ECAL}}/E = (90 \pm 0.1)\%/\sqrt{E} \oplus (4.8 \pm 0.1)\%.$$

For the case of all pions we have

$$\sigma_E^{\text{all } \pi}/E = (77 \pm 0.1)\%/\sqrt{E} \oplus (5.5 \pm 0.1)\%.$$

At low energies the energy resolution of all pions is narrower than pions which are mip in ECAL due to the fine sampling of the ECAL calorimeter.

Figure 9 and Figure 10 show the linearity and resolution of the PbWO<sub>4</sub> crystal configuration for hadrons mip in ECAL and all hadrons. Hadrons mip in ECAL have the same linearity

and resolution in both configurations. However, the  $\text{PbWO}_4$  crystal data for all pions ( $\alpha=1$ ) is non-linear. The average response of the combined ECAL+HCAL calorimeter to pions is also approximately 10% lower than the HCAL only calorimeter. The resolution is much worse for all pions than pions mip in ECAL. The linearity and resolution is shown for  $\alpha=1.4$ . Although both the linearity and resolution are improved, this type of energy sum cannot be used for jets.

Figure 11 shows the scatter plot of the total energy response of the calorimeter normalized the beam momentum,  $E_{TOT}/p_{beam} = (E_{EM} + E_{HAD})/p_{beam}$  as a function of the fraction of energy deposited in the ECAL,  $f_{EM} = E_{EM}/(E_{EM} + E_{HAD})$ . Data points with  $f_{EM} \approx 0$  correspond to pions that interacted in the HCAL. Data with  $f_{EM} \approx 1$  correspond to pions fully contained in the ECAL. A fit of the data binned as a function of  $f_{EM}$  to a second degree polynomial is shown on the figure. The fitted function  $corr(f_{EM})$  is used to correct the total energy.

$$E_{TOT}^{cor} = (E_{EM} + E_{HAD})/corr(f_{EM})$$

The linearity and resolution are shown on Figure 9 and 10 for the  $f_{EM}$  corrected data. The correction improves the linearity and resolution.

## REFERENCES

1. V.I. Kryshkin and A.I. Ronzhin, Nucl. Instrum. Methods, **A247** (1986) 583.; M.G. Albrow et al., Nucl. Instrum. Methods, **A256** (1987) 23
2. G.W. Foster, J.Freeman, and R.Hagstrom, Nucl. Phys. B, **A23** (1991) 93; P. de Barbaro et al., Nucl. Instrum. Methods, **A315** (1992) 317; P. de Barbaro and A. Bodek, A Compilation of Tile/Fiber R&D Results, University of Rochester Preprint UR-1389 (1994)
3. C. Swenberg and N.E. Geacintov, Organic Molecular Photophysics, Vol I, J. Birks, ed., J. Wiley and sons, New York, 1973
4. J. Freeman, The CMS Central Hadron Calorimeter, Proc. VI International Conference on Calorimetry in High-Energy Physics, Frascati, Italy, June 8-14, 1996

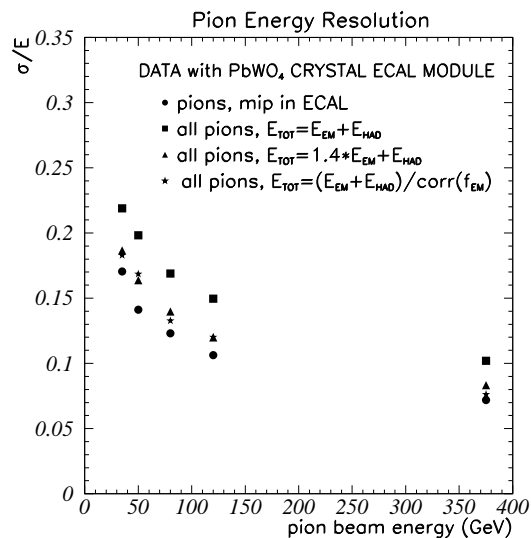


Figure 10. Resolution of of  $\text{PbWO}_4$  crystal ECAL module for hadrons.

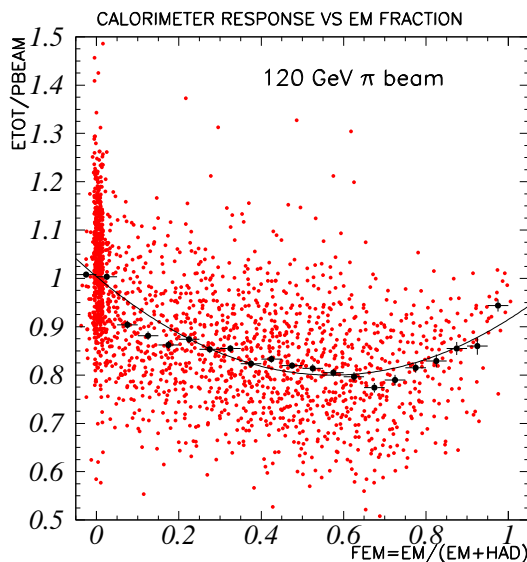


Figure 11. Energy response to pions, as a function of ECAL fraction for the  $\text{PbWO}_4$  crystal ECAL module.